

A comparative 3D simulation approach with extensive experimental Vt/Avt data and analysis of LER/RDF/reliability of CMOS SRAMs at 40-nm node and beyond

Takako Okada

Corporate Research & Development Center
Toshiba Corporation
Kawasaki, Japan
takako.okada@toshiba.co.jp

Hisao Yoshimura, Hisashi Aikawa, Mitsuhiro Sengoku
Osamu Fujii and Hisato Oyamatsu
System LSI Division, Semiconductor Company
Toshiba Corporation
Ohita, Japan

Abstract— With the advent of CMOS SRAMs manufactured at 40-nm node and beyond, variability of threshold voltage (Vt) and technology-dependent factor in Pelgrom plot (Avt) has become a serious issue in the practical design and fabrication phases. This paper presents (i) a comparative 3D simulation approach using extensive measured data to clarify the magnitudes of LER and RDF effects in generic processes, (ii) estimation of magnitudes of LER, RDF and FER (metallurgical junction front edge roughness) effects, (iii) simulation of LER, RDF and FER in a FinFET device to evaluate practical feasibility and (iv) analysis of size-dependent NBTI-induced Vt fluctuation as a possible application of this method.

I. INTRODUCTION

The continuous miniaturization of CMOS SRAMs down to 40-nm node has led to significant changes in process and device design, and has made variability and reliability issues crucial^{[1]-[3]}. The importance of Vt roll-off and Avt control has increased greatly in the actual design and fabrication phases. We have proposed a comparative 3D simulation approach using extensive measured data, and have clarified the magnitudes of LER and RDF effects in generic processes. We used this approach in actual practice to evaluate LER/RDF effects and to provide practical feedback. In order to do this, we paid special attention to (1) net number and spatial distribution for the impurities and trap site, (2) regridding around the metallurgical junctions to preserve the fluctuation, and (3) intensive optimization of process models.

II. FLOW OF COMPARATIVE 3D SIMULATION APPROACH

The flow of the comparative 3D simulation approach is presented in Fig. 1. With regard to impurity and trap site distributions in scaled devices, in addition to the random location it is necessary to pay attention to net-number fluctuation. It is noticed that the net-number of impurities is definitely fluctuated in individual area, particularly in the halo region as can be seen in the figure. Basic frame of simulation tool which we used is 3D Sentaurus process/device produced by Synopsys.^[4] Before using the

process simulator in actual practice, we intensively examined experimental data for B, As, P, In, and Ge from more than 60 sources in the literatures^[5] and we optimized models for scaled device design phase. We implemented LER model based on Kaya's method^[6]. We also confirmed that the results produced by our random-number-based variability simulator were consistent with the results of our experimental data acquisition procedure (eqs. 1 and 2) as shown in Fig. 2, where P means an observable and herein the value is a threshold voltage Vt of transistor. The value of ΔP is a difference of Vts in an adjacent neighbor pair of transistors. L, W and D are channel length, channel width and distance in neighbor pair

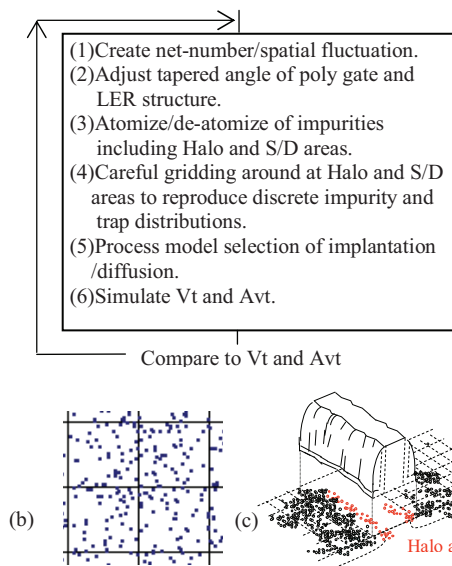


Fig.1 Schematic illustration of comparative 3D simulation approach. (a) Successive simulations are done with tuning of items (1) to (6) until obtaining well-reproduced results. (b) net-number/spatial fluctuation for impurity and hole trap, and (c) typical image of discrete atoms around at Halo and S/D edge areas.

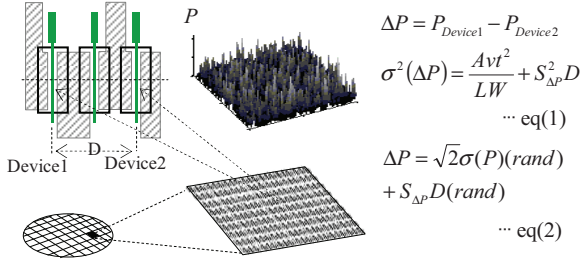


Fig.2 Procedures of variability measurements on paired transistors over whole wafers. Simulation results using random number have been checked to be consistent to experimental procedures.

transistors, respectively. Moreover, Avt which we focus is a linear coefficient of Pelgrom plotting.

III. SHIMULATED AVT, METALLUGICAL JUNCTION FRONT EDGE ROUGHNESS AND FEASIBILITY STUDY OF FIN DEVICES

We would like to herein report our simulated characteristics of Avt, junction edge roughness, feasibility study of Fin devices and preliminary work of size dependent NBTI-induced V_t behaviors using our comparative 3D simulation approach.

A. V_t roll-off and Avt characteristics

As a part of variability work, we have studied V_t roll-off simulation in terms of process models by two- and three-dimensional executions. The typical simulated V_t for saturation regions are plotted for various adopted models with experimental data in Figs. 3(a) and 3(b). As can be seen, the V_t roll-off characteristics depend on adopted models and reproduce well experimental data together with LER/RDF models and Monte Carlo ion implantation model. Moreover, it is understood from Fig. 3(b) that two-dimensional calculation (blue diamond symbol) can not trace the roll off at all.

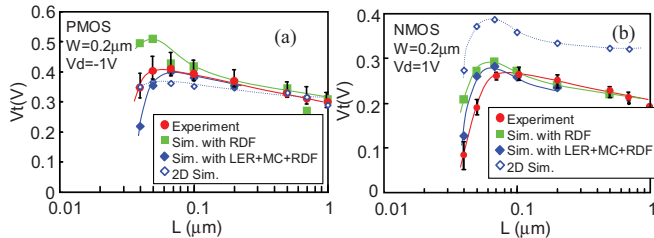


Fig.3 V_t roll-off in terms of adopted models for (a)PMOS and (b)NMOS in saturation region. Each symbol on observed curves stands for value averaged over 40 experimental points.

We have also intensively examined individual impurity distribution with three dimensional visual aids. Fig. 4 shows the simulated impurity distributions for various adopted models. Fig. 4 (a) shows a result with taking into accounts of both RDF, LER and Monte Carlo ion implantation. Some parts of channel areas are observed narrower which result in V_t roll-off as reported in Fig. 3. As shown in Fig. 4(b), front edge of metallurgical junctions has become rough caused by RDF effect though the gate line edge is straight completely. The FER effect increases the variability similarly to LER.

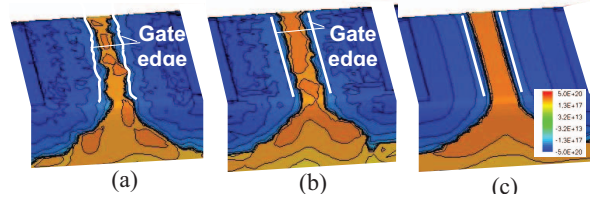


Fig.4 Typical simulated impurity distributions underneath gate area (a) taking into accounts of both RDF, LER and Monte Carlo ion implantation., (b) RDF, and (c) continuum models. L_{poly} is of 40 nm.

The values of the standard deviation of threshold voltage (σV_t) are plotted in Fig. 5. A value of Avt is a linear coefficient shown in the inset of the figure.

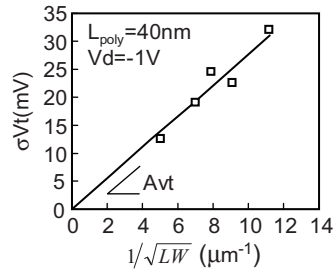


Fig.5 Typical Pelgrom plot of simulated threshold voltages.

Avt values are important indices for scaled CMOS SRAM. We have studied Avt characteristics in both linear and saturation regions for PMOS and NMOS. Hereupon, we have focused on saturation region characteristics, since LER, RDF and FER effects would be markedly appeared in device behaviors. The simulated Avt-L_{poly} characteristics for PMOS are shown in Fig. 6 for the different models together with experimental data. The L_{poly} length(L) and the channel width(W) were varied from 40 nm to 1 μm and 0.2 μm to 2 μm, respectively. It has been observed from the experiment that Avt data depend on L_{poly} definitely. Comprehensive comparison of the simulated and experimental results revealed that RDF effects in halo region caused by discrete impurity atom fluctuations are dominant in Avt variability over a range of L_{poly} of 0.1 to 1 μm. In the shorter L_{poly} range of 40 nm to 0.1 μm, it was revealed that FER effect and local dose fluctuations of halo implantation process overlay on RDF effect. As a result, the Avt value increases with decrease in

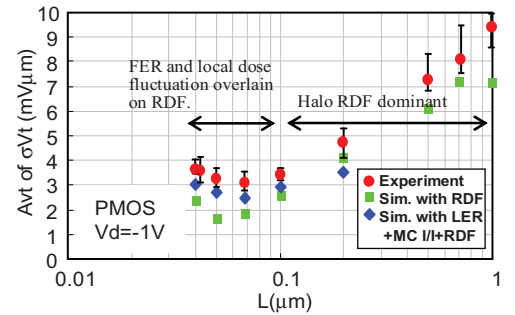


Fig.6 Avt characteristics of σV_t in PMOS. The standard deviation of LER is of 2nm. Simulations have been done with three dimensional.

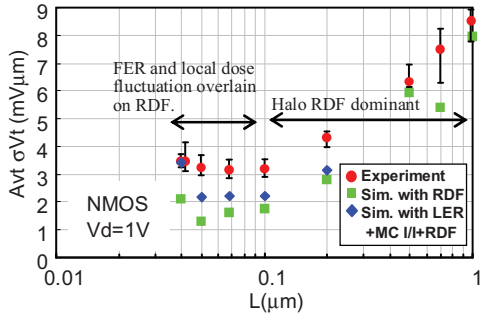


Fig.7 Avt characteristics of σV_t in NMOS.

L_{poly} as can be seen in Fig. 6. We can also discuss same analogy to NMOS, however, there is still a small discrepancy between simulated and experimental results as shown in Fig. 7. In order to improve the discrepancy, we have studied intensively several features such as (i)to develop precise tilted BF₂ implantation and dissociation models, (ii)to observe precise gate edge structures in especial NMOS with n⁺ recrystallized poly-silicon involving various orientations, and (iii)to estimate work function variability caused by recrystallized poly silicon orientation fluctuation in NMOS.

B. Feasibility study of Fin devices and size dependent NBTI-induced V_t fluctuation

Fin device is one of promising candidates for 32- to 22-nm-node CMOS SRAMs. Employing a typical published process^[7], we used our simulation tool to evaluate LER, RDF and FER effects. Fig. 8(a) shows a typical intermediate output structure of FinFET SRAM cell in which we can see narrow

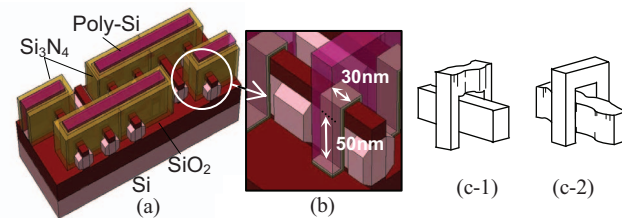


Fig.8 FinFET structure for simulation. (a) Snap shot of cell structure for ion implantation process, (b) magnification of Fin devices, (c-1) gate LER, and (c-2) Fin LER.

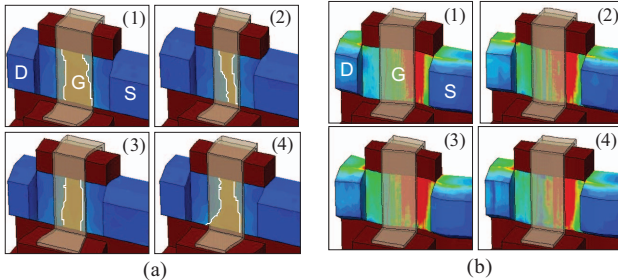


Fig.9 Typical four simulated results of LER and RDF. (a)Impurity distribution at S/D in case c-1, and (b)current distribution for saturation conditions in case c-2.

walls of poly-Si/Si₃N₄. We have carefully optimized ion implantation process, particularly to S/D areas in a whole process sequence of Fin SRAM, because ion implantation angle margins (tilt and rotation angles) are markedly limited due to tall photo resist walls. Some of dimensions of the Fin are listed on Table 1. A magnification of the transistor is given on Fig. 8(b). We have examine two kinds of LER; gate LER shown in Fig. 8(c-1) and Fin LER in Fig. 8(c-2). Typical four simulated results of impurity distributions with the gate LER are shown in Fig. 9(a), where S/D metallurgical junction front edges have been seen. 3D current distributions are also given on Fig. 9(b) for four typical Fins with the Fin width LER. Summary is listed on Table 1. Although junction front edge roughness has been seen in Fig. 9(a), variability of V_t have been improved on both gate LER and Fin LER shown in Table 1. The V_t variability characteristics could be interpreted in terms of well-controllability of current by dual gate in Fin device.

Table 1 Comparison of simulated results of Fin device with planar device. Simulation has been done at $V_d=1.0V$. Symbol of * stands for mean value.

	Fin FET	Planar MOS
L	30nm	40nm
W	50nm×2	0.2μm
Fin width	20nm	-----
Channel concentration	1e18 /cm ³	2e18/cm ³
Gate LER +RDF	σV_t : 30mV(0.31V)* σI_{on} : 3.6μA(72.1μA)* σI_{off} : 4.4e-11A(2.7e-11A)*	34mV(0.17V)* 5.5μA(106μA)* -----
RDF	σV_t : 15mV(0.35V)*	27mV(0.495V)*
Gate LER	σV_t : 22mV(0.35V)*	-----
Fin LER	σV_t : 12mV(0.35V)*	-----

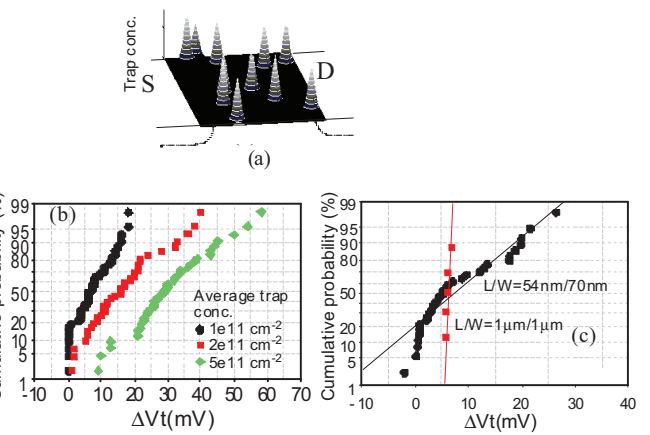


Fig.10 NBTI results for PMOS stressed with $V_{gs}=-1.4V$ and $V_d=0V$ at 125°C. (a) Net-number/spatial fluctuation for hole trap, (b) preliminary simulation results for three different stress durations($L/W=40nm/0.2mm$), and (c) experimental results of size dependence of V_t degradation.

NBTI(negative bias temperature instability) is one of major issues in scaled CMOS SRAM. Several works such as physical NBTI mechanism discussion, process feedback for

dielectric film improvements and so on have been already reported in many literatures^[8]. Herein we have focused on size dependence of NBTI-induced V_t degradation fluctuation estimation from a view point of device reliability. We have called upon our tool with net-number/spatial fluctuations of impurity and trap sites for this job. We have simulated fluctuation of V_t degradation (σ_{Vt}) on the assumption that both hydrogen passivation and depassivation reactions are Poisson processes^[9]. As shown in Fig. 10(a), traps have been scattered at channel area based on the net-number and the spatial fluctuation functions. Preliminary results of σ_{Vt} variability in a small device of $L/W=40\text{nm}/0.2\mu\text{m}$ are shown in Fig. 10(b), which can be seen reproduced well qualitatively the experimental curve of small size device of $L/W=54\text{nm}/70\text{nm}$ shown in Fig. 10(c). Using this simulation procedure in conjunction with LER/RDF/FER effects, we could predict more realistic NBTI-induced V_t variability and also discuss reliability including worst-case scenario of scaled CMOS SRAM.

IV. SUMMARY

We have presented a comparative 3D simulation approach based on extensive measured V_t/Avt data in order to evaluate LER/RDF/FER effects in actual practice and to provide feedback. Through intensive examinations of impurity implantation/diffusion models and customizations and creation of net-number/spatial fluctuation, we have reproduced well V_t/Avt characteristics and have discussed individual magnitude of LER/RDF/FER effects. Moreover, we have reported variability of Fin device as one of promising candidates for 32- to 22-nm-node CMOS SRAMs. Furthermore, using our three dimensional tools with net-number/spatial fluctuations of impurity and defect sites, we have simulated size dependent NBTI-induced V_t fluctuation as a possible application for device reliability

V. ACKNOWLEDGE

We would like to express our special gratitude to Dr. F. Matsuoka, Dr. A. Nishiyama and Dr. J. Koga of Toshiba Corporation for valuable suggestions towards our work.

REFERENCES

- [1] M. J. M. Pelgrom, A. C. Duinmaijer and A. P. G. Welbers, ‘Maching properties of MOS transistors’, IEEE J. Solid-State Circuit, vol. 24, no. 5, (1989) pp. 1433-1440.
- [2] A. Asenov, S. Kaya and J. H. Davies, ‘Intrinsic threshold voltage fluctuations in decanano MOSFETs due to local oxide thickness variations’, IEEE Trans. Electron Devices, vol. ED-49, no. 1, (2002) pp. 112-119.
- [3] K. Takeuchi, T. Tatsumi, and A. Furukawa, ‘Channel enginnering for the reduction of random dopant placement induced threshold voltage fluctuation’, IEDM 1997, pp. 841-844.
- [4] Sprocess and sdevice system user guides, v-a2008.09 Synopsys Inc., CA, USA.
- [5] For examples of checking with diffusion data, F.Morehead, R.Young, D.Chidambaram, C.Murthy, P.Murley, and S.Fischer, ‘Modeling and calibration of TED’, p.127, and others in Process physics and modeling in semiconductor technologies, ed. G.R.Srinivasan Electrochem. Society Proc. vol.PV. 96-4. For examples of cheking with co-implantation data, Y.Chen, B.Obradovic, m.morris, G.Wang, G.Balamurugan, D.Li, A.F.Tasch, D.Kamenitsa, W.McCoy, S.Baumann, R.Bleier, D.Sieloff, D.Dyer, and P.Zeitzoff, ‘Physically based models for indium and germanium ion implantation into silicon’, p.33, and others in Process physics and modeling in semiconductor technologies, ed. C.S.Murthy, vol.PV 99-2.
- [6] S. Kaya, A. R. Brown, A. Asenov, D. Magot and T. Linton, ‘Analysis of statistical fluctuations due to line edge roughness in sub-0.1um MOSFETs’, SISPAD 2001, pp. 78-81.
- [7] H. Kawasaki, M.khater, M. guillom, N. fuller, J.Chang, S.K. Kanakabapathy, L.Chang, R.Muralidhar, K.Babich, Q.Yang, J.Ott, D.Klaus, E.Kratschmer, E.Sikorski, R.Miller, R.Viswanathan, Y.Zhang, J.Silverman, Q.Ouyang, A.Yagishita, M.Takayanagi, W.Hsensch, and K.Ishimura, ‘Demonstration of highly scaled Fin fet SRAM cell with high-k metal gate and investigation of characterisit variavility for the 32nm node beyond’, IEDM 2008, pp. 237-240.
- [8] As some of examples of technical and physical overviews, Chapter 2 NBTI in high-k gate dielectrics, by M.Housa, p.359, and Chapter 4 Toward enginnering mdeling of NBTI, by Grasser, p.399, in Defects in microelectronic materials and devices, Ed. D.M.Fleewood, S.T.Pantelides, and R.D.Schrimpf, CRC Press, 2010. ISBN 978-1-4200-4376-1
- [9] S. E. Rauch III, ‘Review and reexamination of reliability effects related to NBTI-induced statistical variations’, IEEE Tran. Device Mater. Rel., vol.7, no.4, (2007) pp. 524-530.